Precision Engineering 47 (2017) 452–458

Contents lists available at ScienceDirect

Precision Engineering

journal homepage: www.elsevier.com/locate/precision

Design of high-precision ball screw based on small-ball concept

Tetsuya Miura [a,*], Atsushi Matsubara [b], Daisuke Kono [b], Kazuma Otaka [b], Kaoru Hoshide [c]

[a] Engineering Division, THK Co., LTD., 754 Nakadate Chuo-shi Yamanashi, 409-3801 Japan
[b] Department of Micro Engineering, Kyoto University, Katsura Nishikyo-ku, Kyoto, 615-8540 Japan
[c] Engineering Division, THK Co., LTD., 4-9-16 Higashikoujiya Ota-ku, Tokyo, 144-0033 Japan

ARTICLE INFO

Article history:
Received 14 June 2016
Received in revised form 8 August 2016
Accepted 6 September 2016
Available online 1 October 2016

Keywords:
Ball screw
Drive
Servo system
Position deviation
Torque fluctuation

ABSTRACT

This paper addresses a design method of ball screws for high-precision feed drives of machine tools. The torque fluctuation of a ball screw influences position deviation, which deteriorates the contorting accuracy. The torque fluctuation comes from the load change of the contacting balls between the nut and the screw shaft during ball circulation. In order to decrease the load change, a ball screw that employs smaller balls was designed and evaluated in the measurement tests. The experimental results showed that the designed ball screw could decrease both the torque fluctuation and position deviation.

1. Introduction

Feed drives are key elements that dominate the motion speed, stiffness, and accuracy of machine tools. The moving object (table, column, saddle) is driven by a linear motor, or a rotary servomotor via a ball screw [1]. The linear motor can drive the table directly at high speed (e.g., 240 m/min) and reduce positioning time under the high gain servo system [2]. However, in the case, where a large driving force is required, the required motor size becomes larger, thus increasing the difficulty in machine design and increasing machine cost. Therefore, linear motor drives are used in relatively small high-precision machines [3] and ultra-precision machines [4–6]. In contrast, ball screw drives are widely used for many types of machine tools. Using the ball screw, the combinations of force and feed speed could be flexible based on the lead of the screw. Additionally, the ball screw is compact, and the total cost of the drive system is not high.

In spite of the above-mentioned advantages, the application of the ball screw to high-precision machine tools is difficult. One of the problems is that the ball screw itself has flexible elements, balls and a screw shaft. To avoid axial vibration due to the flexibility, Erkorkmaz proposed vibration cancelation techniques such as notch-filter, adaptive sliding mode control [7], and active damping control [8]. Pritschow and Croon proposed re-design of the support-bearing unit to have lower stiffness and higher damping [9]. To increase the robustness, Gordon applied the pole placement and loop shaping to enhance the disturbance rejection function [10].

It is widely known that rolling elements in the ball screw and linear motion guideway have nonlinear relationships between the tangential friction force and the displacement. As the characteristic causes quadrant errors in circular motion, many compensation models have been studied [11]. Fukada et al. measured nonlinear elastic behavior of the ball screw using an original experimental apparatus and interpreted the measurement results into a viscous-elastic-plastic model [12]. To increase the stiffness of a ball screw, Verl proposed an adjustment mechanism consisting of nut preload [13]. Feng proposed a measurement method using an acceleration sensor to investigate preload variation of a ball screw [14].Guevarra et al. used a lapping process for the groove surfaces of screw shafts in order to improve travel variation and drunkenness [15]. There are much research regarding friction compensation, preload, and stiffness design of ball screws, however there is no significant research on avoiding the friction fluctuations that occur due to translation mechanisms and influence the servo errors.

In this research, the torque fluctuations of a ball screw and position deviations were measured using a torque measurement device and a test drive with an aerostatic guideway, and the position deviations were analyzed using the method proposed by Kono et al. [16]. Based on the analysis of the relation between the torque fluctuations and the position deviations, the load variation in the ball screw due to the ball circulation was targeted to be decreased. Ball

* Corresponding author.
E-mail address: te.miura@thk.co.jp (T. Miura).

http://dx.doi.org/10.1016/j.precisioneng.2016.09.020
0141-6359/

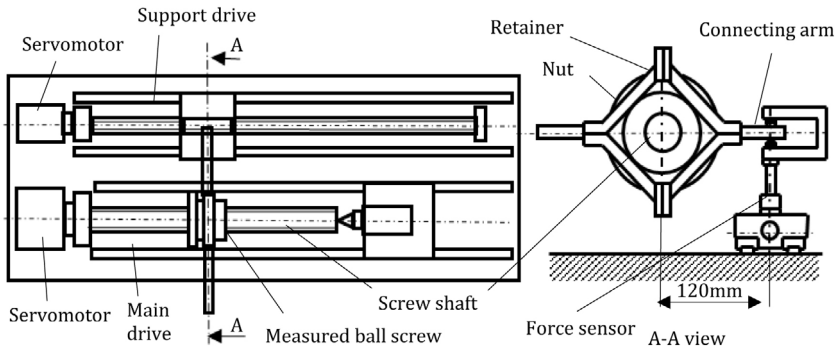

Fig. 1. Torque measurement devise.

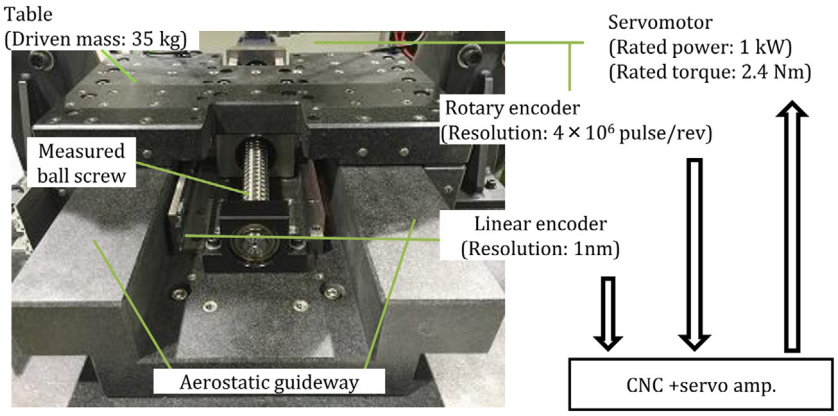

Fig. 2. Test drive for measurement of position deviation.

screws were designed using smaller balls (small-ball concept) and evaluated in the measurement tests.

2. Experimental analysis

2.1. Measurement method

Fig. 1 shows a measurement device for the analysis of a friction torque of a ball screw. A ball screw to be measured is rotated with a servomotor in a main drive. The rotation of the nut is constrained by a retainer, which is connected to the supporting drive with an arm. The main drive and the supporting drive move synchronously, which allows the nut to move on the screw shaft. A force sensor is installed at the end of the connecting arm, which measures the force required for the nut to resist rotation. The friction torque is estimated by multiplying the measured force and the distance between the centers of the two drives (120 mm). The friction torques were measured in backward and forward motions and repeated three times. Preload torque was adjusted at 0.12 Nm based on the ISO3408-3 [17]. Torque fluctuation was evaluated at a rotation speed of 15 min^{-1}.

Fig. 2 shows a test drive used to measure the position deviation in control motion. The ball screw, rotated by a servomotor, drove the table supported by a friction-less aerostatic guideway. The ball screw was mounted on the test drive, while keeping the runout of the shaft end within 3 μm and the parallelism between the screw shaft and the guideway within 10 μm.

For feed control, a market CNC controller with a drive amplifier was used. The control system employs a cascade of current-velocity-position loops. The block diagram is shown in Fig. 3. The motor position was detected by a rotary encoder for velocity loop, and the table position was detected by a linear encoder for position

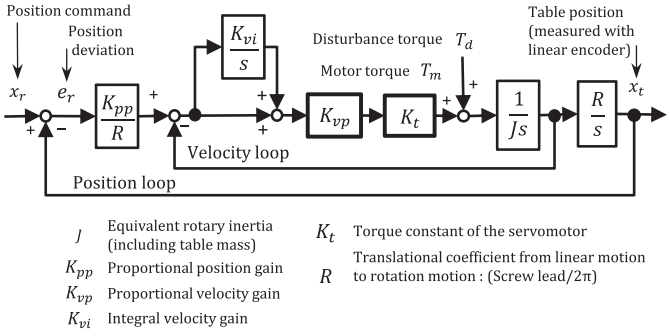

Fig. 3. Block diagram of the servo system.

loop. The position deviation (shown as e_r in Fig. 3) was logged using the measurement function of the CNC. Servo gains were set so that the velocity open loop had a gain margin of 10 dB and a phase margin of 40°. The bandwidth of the velocity feedback loop ω_{vc} [rad/s] is as follows:

$$\omega_{vc} = \frac{K_{vp} \cdot K_t}{J} \tag{1}$$

There exist notch filters in the velocity loop, which mainly suppress the torsional vibration resonance. The feed speed was selected from 120 mm/min to 3000 mm/min. Sampling period was set to 0.18 ms. The travel distance was set at 120 mm and the travel round-trips was 2 times. Analysis area of the position deviation was 80 mm to remove the areas of both ends 20 mm in order to steady-state velocity conditions.

Table 1
Specification of ball screw A.

Screw shaft outer diameter	32 mm
Ball-pith-circle diameter, d_m	33.25 mm
Lead, l	8 mm
Ball diameter, D_w	4.763 mm
Lead angle, φ	4.38°
Nut outer diameter	58 mm
Nut overall length	42.5 mm
No. of loaded circuits (Rows × Turns × threads), i	1 × 2 × 1
Number of effectively loaded balls, Z	39
Contact angle, α	43°
Basic dynamic axial load rating, C_a	11,422 N
Basic static axial load rating, C_{0a}	26,086 N
Preloading type	Over size ball
Preload	570 N (5%C_a)
Preload torque	0.12 Nm

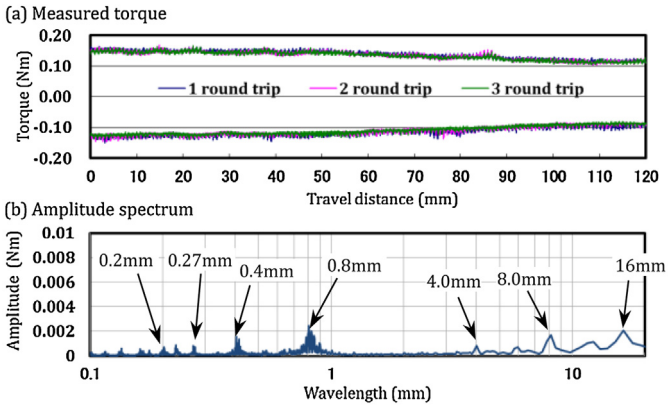

Fig. 4. Measured friction torque and amplitude spectrum (ball screw A).
(a) Measured torque. (b) Amplitude spectrum.

2.2. Measurement result

Table 1 shows the specification of a sample ball screw (referred to as ball screw A). The ball screw employs over-sized-ball preloading and a lead of 8 mm. The friction torque of the ball screw was measured using the torque measurement device. Fig. 4 shows measured friction torque and its amplitude spectrum with respect to the wavelength of the travel distance. As seen in Fig. 4(b), the friction torques involve variations with wavelengths of 4.0, 8.0, 16 mm, which are related to the lead of the screw. There also exist higher order variations with wavelengths of 0.2 and 0.27, 0.4, 0.8 mm.

The wavelengths can be explained by using the following formulas. Assuming that the ratio of ball revolution to the shaft rotation is ε and the ball-pith-angle in the loaded circuit of nut is θ_b [rad], these are given by the following formulas, respectively [18].

$$\varepsilon = \frac{1}{2}\left(1 - \frac{D_w \cdot \cos\alpha}{d_m}\right) \tag{2}$$

$$\theta_b = 2\sin^{-1}\left(\frac{D_w \cdot \cos\varphi}{d_m}\right) \tag{3}$$

The parameters in Eqs. (2) and (3) are explained in Table 1. The wavelength that is related to the ball circulation, λ_b [mm] can be written as

$$\lambda_b = \frac{\theta_b \cdot l}{2\pi\varepsilon} \tag{4}$$

Using the values in Table 1, λ_b is calculated as 0.8 mm for ball screw A, which corresponded to the wavelength of measured torque fluctuation. The wavelengths of 0.2, 0.27, and 0.4 mm are considered as higher harmonic components.

The position deviation was measured using the test drive shown in Fig. 2. The servo gains were tuned as

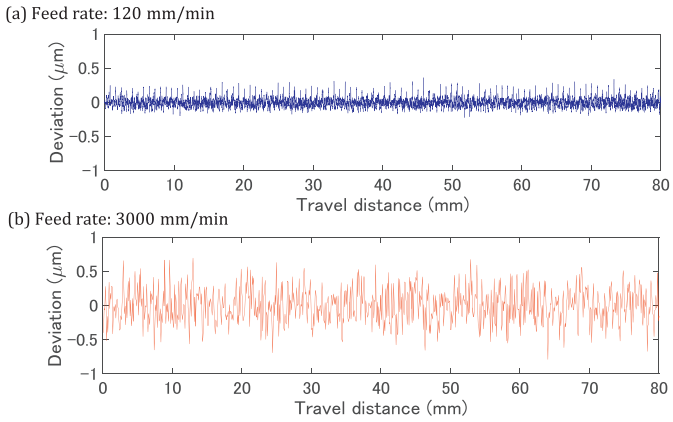

Fig. 5. Measured position deviations (ball screw A).
(a) Feed rate: 120 mm/min. (b) Feed rate: 3000 mm/min.

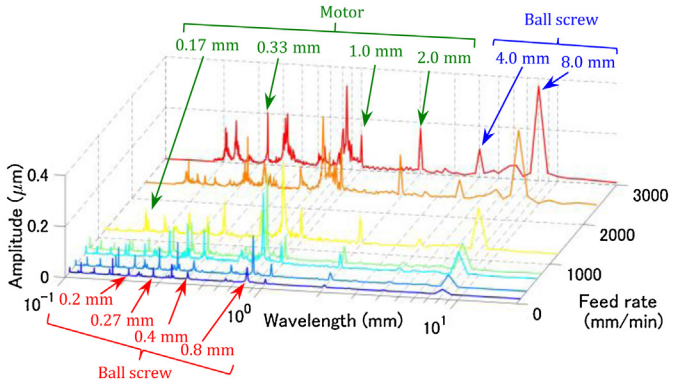

Fig. 6. Amplitude spectra of position deviation (ball screw A).

ω_{vc} = 790 rad/s, K_{vi} = 130 rad/s, K_{pp} = 79 rad/s. Fig. 5 shows two examples measured at low speed (120 mm/min) and high speed (3000 mm/min). The P-V values of position deviations were 0.6 μm at feed speed 120 mm/min and 1.6 μm at feed speed 3000 mm/min, respectively. As can be seen in these figures, the position deviation increases as the speed increases and has several periodic components. Amplitude spectrum was obtained using Fourier transfer. These results are summarized in Fig. 6. Note that when the feed rate is more than 2400 mm/min, wavelengths less than 0.2 mm could not be analyzed due to limitation of the sampling time. In Fig. 6, each wavelength doesn't seem to change for different feed rates. This implies that the variations are not time-dependent but position-dependent. Further, it can be seen that the amplitudes change because of the feed rate. For example, the amplitudes with the wavelengths of 4.0 and 8.0 mm decrease with a decrease in the feed rate. The amplitudes with the wavelengths of 0.2, 0.27, 0.4, 0.8, and 4.0, 8.0 mm were observed in Fig. 6. As these wavelengths agree with the results in the torque measurement, these must come from the ball screw. There also existed the amplitudes with wavelengths of 0.17, 0.33, 1.0 and 2.0 mm, which may come from the servomotor.

To confirm it, the position deviation of the servomotor, which was separated from the ball screw and controlled by the semi-closed control was measured with the rotary encoder. The servo gains were decreased to 1/3 to avoid control instability. Fig. 7 shows the wavelength analysis of the measured position deviations. The amplitudes with wavelengths of 0.17, 0.33, 1.0 and 2.0 mm could be found in the position deviations of the servomotor.

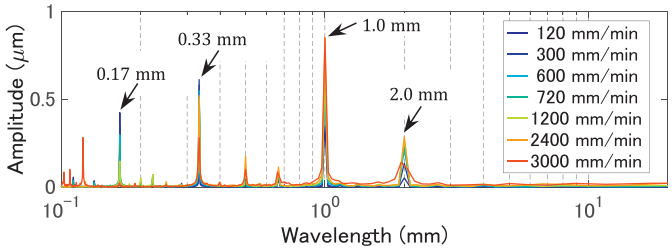

Fig. 7. Amplitude spectra of position deviation (Only the servomotor).

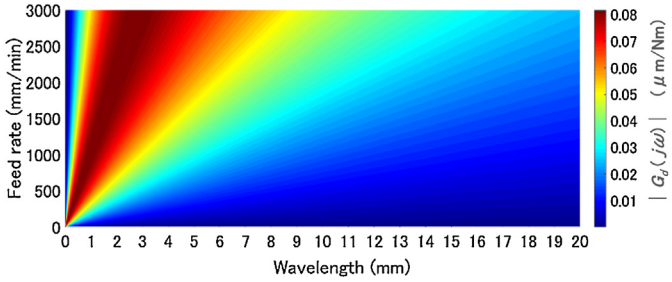

Fig. 8. Disturbance rejection function.

3. Ball screw design

3.1. Disturbance rejection of servo system

The position-dependent variation in torque behaves as periodic disturbance to the servo system. The disturbance rejection of the servo system could be estimated from the transfer function from T_d to x_t in Fig. 3.

$$G_d(s) = \frac{Rs}{Js^3 + K_{vp}K_t s^2 + \left(K_{pp}K_{vp}K_t + K_{vi}K_{vp}K_t\right)s + K_{pp}K_{vi}K_{vp}K_t} \quad (5)$$

Assume that the wavelength of the torque fluctuation is λ [mm], the feed rate is F_s [mm/min], and the excitation angular frequency is ω [rad/s]. Then, the following relation holds:

$$\omega = \frac{2\pi F_s}{60\lambda} \quad (6)$$

Using this relation, the sensitivity and gain $|G_d(j\omega)|$ with respect to the wavelength and the feed rate are calculated and shown in Fig. 8. The figure indicates that the variation with the wavelength around 8 mm could be suppressed by the servo system. In contrast, it is difficult to suppress the torque fluctuations with the wavelength 1 mm or less. This result agrees with the amplitude spectra shown in Fig. 6.

3.2. Design with small- ball concept

High-precision parts such as optics parts and dies are machined at feed rates around 500–1000 mm/min in the finishing process. In order to design a ball screw covering this speed range, the torque fluctuations with the wavelength 1 mm or less should be removed. The fluctuations with wavelengths of 0.2, 0.27, 0.4 and 0.8 mm are related to the ball-passing interval. A ball screw nut has return tubes for the balls to circulate. When the balls come in contact with the nut and the screw shaft, the load distribution of the balls changes. Such variation also provides the torque fluctuation. In order to decrease the load variation, smaller balls are applied in our design.

The disadvantage to using smaller balls is that the basic load capacity decreases as the ball size decreases. Based on the ISO 3408-5 [19], the basic dynamic axial load rating C_a [N] and the life L [revolutions] as

$$C_a = f_c \cdot (\cos\alpha)^{0.86} \cdot Z^{\frac{2}{3}} \cdot {D_w}^{1.8} \cdot \tan\alpha \cdot (\cos\varphi)^{1.3} \cdot \left[1 + \left(\frac{C_s}{C_n}\right)^{\frac{10}{3}}\right]^{-0.3} \cdot i^{0.86} \quad (7)$$

$$L = \left(\frac{C_a}{F_m}\right)^3 \cdot 10^6 \quad (8)$$

f_c, C_s and C_n are the coefficients determined by D_w, d_m, α, and the conformity factor in contact. F_m [N] is the axial load added to the nut of the ball screw. Referring Eq. (7), the capacity loss caused by the decrease in the ball size was recovered by increasing Z. To realize this concept, the nut size and the number of loaded circuits were increased.

Table 2
Specifications of ball screw B and C (design by small-ball concept).

	Ball Screw B	Ball Screw C
Screw shaft outer diameter	32 mm	32 mm
Ball-pith-circle diameter, d_m	32.5 mm	32.5 mm
Lead, l	8 mm	8 mm
Ball diameter, D_w	2.381 mm	2.381 mm
Lead angle, φ	4.48°	4.48°
Nut outer diameter	55 mm	55 mm
Nut overall length	42.5 mm	66.5 mm
No. of loaded circuits (Rows × Turns × threads), i	1 × 2 × 2	2 × 2 × 2
Number of effectively loaded balls, Z	160	320
Contact angle, α	43°	43°
Basic dynamic axial load rating, C_a	8259 N	14,990 N
Basic static axial load rating, C_{0a}	27741 N	55,483 N
Preloading type	Over size ball	Over size ball
Preload	413 N (5%C_a)	750 N (5%C_a)
Preload torque	0.09 Nm	0.17 Nm

Table 2 shows the specifications of ball screw B and C designed using the small-ball concept. In both ball screws, the ball size was selected with the diameter of 2.381 mm, and the number of threads was increased to 2. While the number of rows in ball screw B was not changed to keep the nut size, the number of rows in ball screw C was increased to 2 to recover C_a.

The load distributions were calculated based on the normal load of at each contact point of a ball and groove surface [20]. The assumption and procedure for the calculations are as follows.

1) The nut and the screw shaft were rigid-body.
2) The position and the posture of the nut were constrained.
3) In the screw shaft, the rolling in the axial direction was constrained and other degrees of freedom were unconstrained.
4) Each ball was regarded as an elastic body and the preload was applied on the contact surface. The contact was assumed to be Hertzian contact.
5) Equilibrium equations in thee parallel directions and two rotational directions (pitting and yawing) were obtained by integrating the contact loads.
6) Changing the number of balls which are in contact with the screw shaft, the equilibrium equations were solved numerically and the load distributions were obtained.

Fig. 9 shows the calculated load distributions of the balls in the nut. Note that the directions of the ball loads are not shown in this figure. As could be seen in this figure, each ball of ball screw A has a different load at a different position. However, load distributions of ball screw B and C are uniform. A ball at the exit end of the groove goes out and the next ball comes to the end of the groove. In this

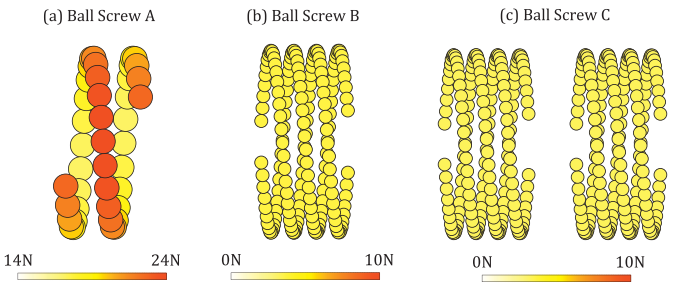

Fig. 9. Load distributions of the balls.

interval the load distribution changes, which produces a total load variation in the axial direction.

This also produces the fluctuation in friction torque. Relationship between the total load in the axial direction and the friction torque is known as

$$T_p = 0.05 \cdot \tan\varphi^{-0.5} \cdot \frac{F_p \cdot l}{2\pi} \cdot 10^{-3}, \tag{9}$$

where T_p [Nm] is the friction torque and F_p [N] is the total load in the axial direction [21].

The load variation due to ball circulation of the conventional ball screw A was calculated as 17.5 N. The load variations of the newly designed ball screw B and C were calculated as 5.0 N and 9.0 N, respectively. Thus, the load variations were decreased less than half in new design. The torque fluctuations were calculated from Eq. (9) by substituting the calculated load variations into F_p. The torque fluctuation of ball screw A was 0.004 Nm, which is almost equal to the measured amplitude shown in Fig. 4. The torque fluctuations of ball screw B and C were calculated as 0.001 Nm and 0.002 Nm, respectively. Thus, it is expected that the position deviation due to the torque fluctuation could be decreased.

4. Evaluation test

The designed ball screws were evaluated in the same measurement tests described in sec. 2.1. The screw shafts in screw B and C are the same. Fig. 10 shows the results of the torque measurement. The wavelength associated with the ball load variation was calculated as 0.4 mm in the new design using Eqs. (2)–(4) and the parameters shown in Table 2. Compared with the results shown in Fig. 4, the new ball screws have few fluctuations related to the ball circulation. The scales of the fluctuations are smaller than the calculated torque fluctuations shown in sec. 3.2. This may come from that balls in the each circuit don't come in and go out at the same time, which cancels the torque fluctuations. The fluctuation with wavelength amplitude 12 mm was increased. This may be because the increase in ball contact makes the friction more sensitive to the circularity of the groove machined on the screw shaft and the nut.

The ball screw was set to the test drive and the position deviation was measured, where the same servo gains were set. Fig. 11 shows examples of measured deviation. In Fig. 11(a),(b), the P-V values of the position deviation of ball screw B were 0.5 μm at feed speed 120 mm/min and 0.8 μm at feed speed 3000 mm/min, respectively. In Fig. 11(c),(d), the P-V values of the position deviation of ball screw C were 0.4 μm at feed speed 120 mm/min and 0.6 μm at feed speed 3000 mm/min, respectively. Compared with the results shown in Fig. 5, the position deviations of new design ball screws

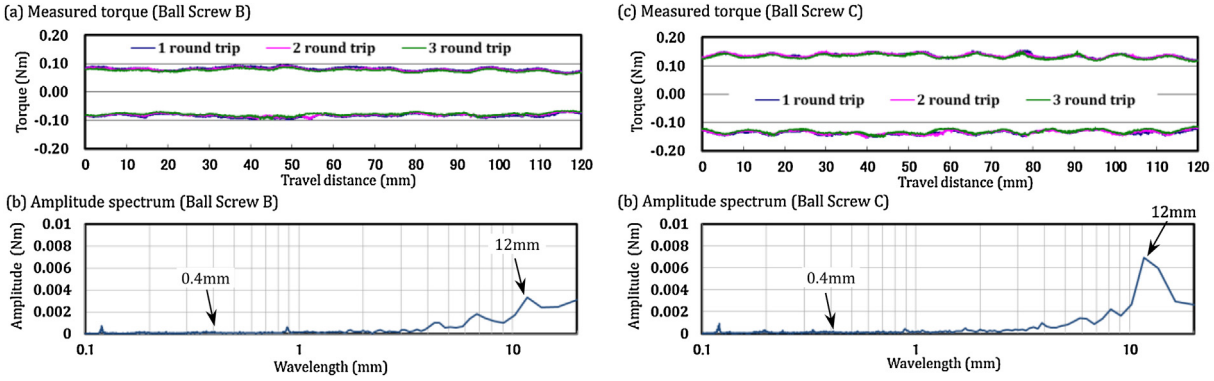

Fig. 10. Measured friction torques and amplitude spectra (ball screw B and C).
(a) Measured torque (ball screw B). (b) Amplitude spectrum (ball screw B). (c) Measured torque (ball screw C). (d) Amplitude spectrum (ball screw C).

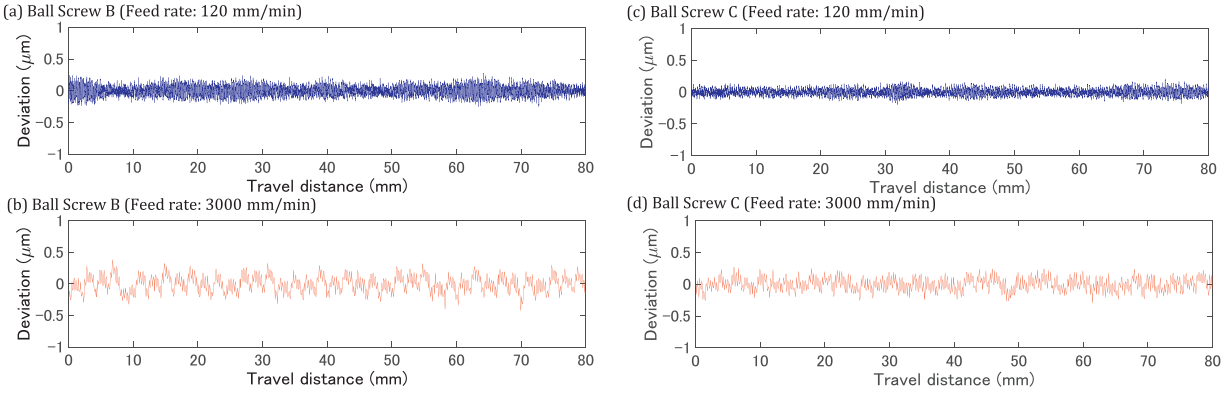

Fig. 11. Measured position deviations of ball screw B and C.
(Feed rate: 120 mm/min and 3000 mm/min). (a) Ball screw B (Feed rate: 120 mm/min). (b) Ball screw B (Feed rate: 3000 mm/min). (c) Ball screw C (Feed rate: 120 mm/min). (d) Ball screw C (Feed rate: 3000 mm/min).

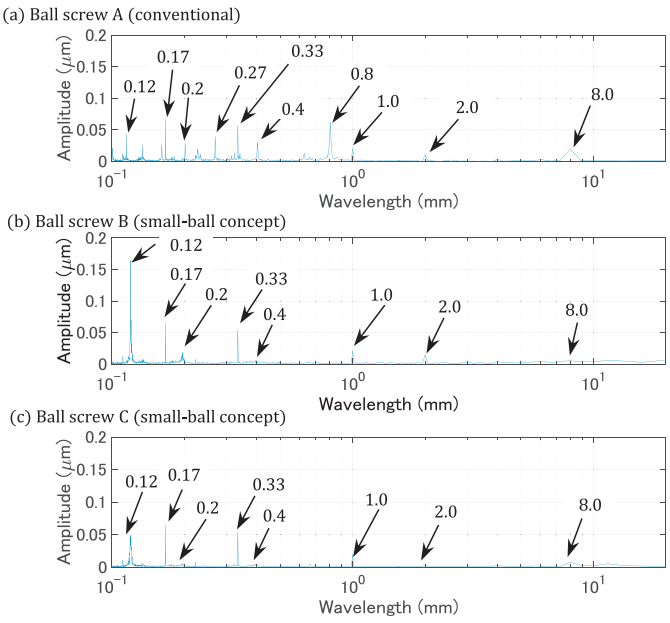

Fig. 12. Amplitude spectra of position deviation (Feed rate: 120 mm/min). (a) Ball screw A (conventional). (b) Ball screw B (small-ball concept). (c) Ball screw C (small-ball concept).

were reduced by 17–63%. Fig. 12(b),(c) show its amplitude spectra (the feed rate is 120 mm/min). For comparison, the amplitude spectrum of ball screw A is also shown in Fig. 12(a). The amplitudes related to the ball circulation in Fig. 12(b),(c) were estimated as 0.2 and 0.4 mm and significantly reduced. There was the amplitude with wavelength 0.12 mm in each ball screw. Fig. 13 shows the measured waviness of the screw shaft which was used for ball screw B and C. The waviness was measured at the ball contact points along groove using an electric micrometer. As seen Fig. 13, the measured waviness involves periodic variations with the wavelengths of 0.12–0.13 mm and 0.06–0.07 mm. It is estimated that the wavelength of 0.12 mm in the position deviation was caused by the waviness of the groove.

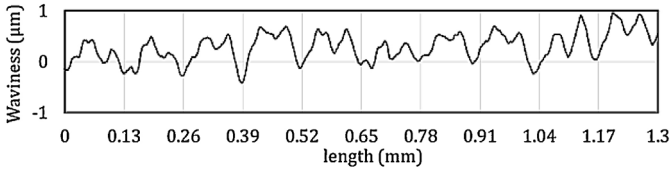

Fig. 13. Measured waviness of screw shaft (ball screw B and C).

Table 3
Measured stiffness of ball screws.

Ball Screw A	Ball Screw B	Ball Screw C
159 N/μm	347 N/μm	632 N/μm

The measurement results in different speeds are summarized in Fig. 14. This figure shows the comparison of the amplitudes categorized in the error resources. As can be seen in this figure, the variation associated with the ball circulation becomes negligibly small. The deviation associated with the screw lead, which was not targeted in our design, increases as the feed rate increases.

The stiffness of the newly designed ball screws were evaluated in the experiment. The ball screw was set to another motion table with linear guideways, which is used for the measurement of stiffness of the ball screw only. The axial load of 500 N was applied to the table using an external loading device with a force sensor. The table positons were measured using two capacitance-type sensors. Table 3 shows the measured stiffness. The newly designed ball screws have 2–4 times larger stiffness than ball screw A. This is because the stiffness is sensitive to the number of loaded balls and less sensitive to ball size (proportional to the power of 2/3).

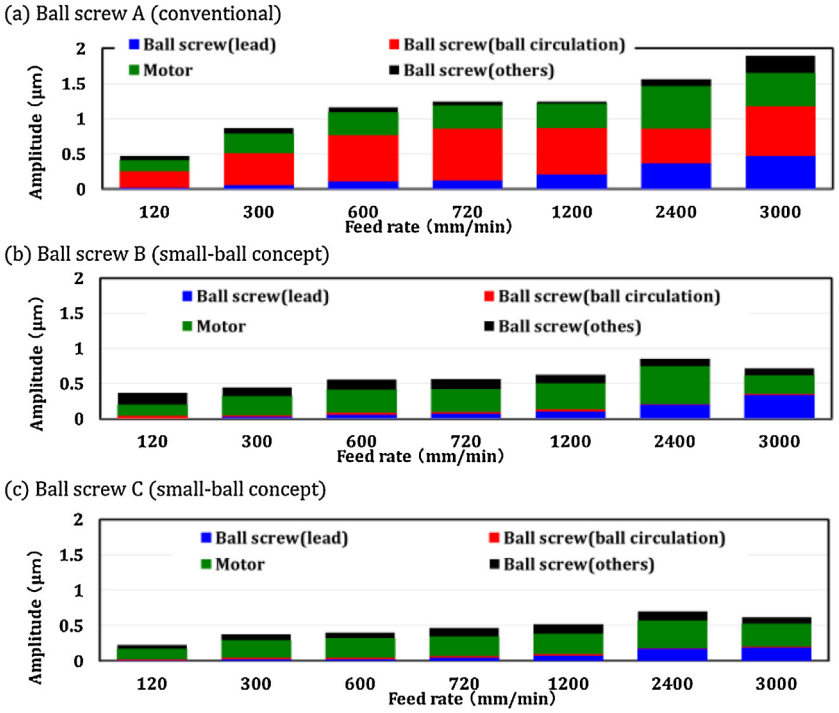

Fig. 14. Deviation amplitudes categorized in components. (a) Ball screw A (conventional). (b) Ball screw B (small-ball concept). (c) Ball screw C (small-ball concept).

5. Conclusions

A high-precision ball screw was designed based on the measurements of friction torques and position deviations. The two ball screws were designed using the smaller balls considering the load variation and evaluated in the measurement tests. The conclusions are summarized as follows.

1 Position deviations were found to be related to torque fluctuations, which depended on the position (rotation). The torque fluctuations were related to the lead and ball circulation of the ball screw. The cascade control system could not suppress the torque fluctuations due to the ball circulation under high gain conditions with the speed range from 120 to 3000 mm/min.
2 The load change in the interval of entrance and exist of balls to the load area was calculated and was used to calculate the torque fluctuation due to the ball circulation. Using smaller balls, ball screws were designed to have smaller torque fluctuations (less than half). Experiment results show that both the torque fluctuations and the position deviations associated with the ball circulation were significantly reduced.
3 The experiment result shows that the stiffness could be increased by 2–4 times owing to the increase of the number of the balls.

References

[1] Altintas Y, Verl A, Brecher C, Uriarte L, Pritschow G. Machine tool feed drives. CIRP Ann—Manuf Technol 2011;60(2):718–79.
[2] Pritschow G. A comparison of linear and conventional electromechanical dives. CIRP Ann—Manuf Technol 1998;47(2):541–8.
[3] Matsubara A, Nagaoka K, Fujita T. Model-reference feedforward controller design for high-accuracy contouring control of machine tool axes. CIRP Ann—Manuf Technol 2011;60(1):414–5.
[4] Takeuchi Y, Kato K, Kawakita S, Sawada K, Sata T. Generation of sculptured surfaces by means of an ultraprecision milling machine. CIRP Ann—Manuf Technol 1993;42(1):611–4.
[5] Sriyotha P, Nakamoto K, Sugai M, Yamazaki K. Development of 5-axis linear motor driven super-precision machine. CIRP Ann—Manuf Technol 2006;55(1):381–4.
[6] Shinno H, Yoshioka H, Taniguchi K. A newly developed linear motor-driven aerostatic X-Y planar motion table system for nano-machining. CIRP Ann—Manuf Technol 2007;56(1):364–9.
[7] Erkorkmaz K, Kamalzadeh A. High bandwidth control of ball screw drives. CIRP Ann—Manuf Technol 2006;55(1):393–6.
[8] Kamalzadeh A, Erkorkmaz K. Compensation of axial vibrations in ball screw drives. CIRP Ann—Manuf Technol 2007;56(1):373–6.
[9] Pritschow G, Croon N. Ball screw drives with enhanced bandwidth by modification of the axial bearing. CIRP Ann—Manuf Technol 2013;62(1):383–4.
[10] Gordon D, Erkorkmaz K. Accurate control of ball screw drives using pole-placement vibration damping and a novel trajectory prefilter. Precis Eng 2013;37(2):308–15.
[11] Brian H, Pierre D, Carlos W. A survey of models, analysis tools and compensation methods for the control of machines with friction. Automatica 1994;30(7):1056–83.
[12] Fukada S, Fang B, Shigeno A. Experimental analysis and simulation of nonlinear microscopic behavior of ball screw mechanism for ultra-precision positioning. Precis Eng 2011;35(4):619–50.
[13] Verl A, Frey S, Heinze T. Double nut ball screw with improved operating characteristics. CIRP Ann—Manuf Technol 2014;63(1):361–4.
[14] Feng G, Pan Y. Investigation of ball screw preload variation based on dynamic modeling of a preload adjustable feed-drive system and spectrum analysis of ball-nuts sensed vibration signals. Int J Mach Tools Manuf 2012;52(1):12–85.
[15] Guevarra D, Kyusojin A, Isobe H, Kaneko Y. Development of a new lapping method for high precision ball screw_1st report feasibility study of a prototyped lapping tool for automatic lapping process. Precis Eng 2001;25(1):63–7.
[16] Kono D, Matsubara A, Shirai T, Hoshide K, Miura T, Togashi T. Analysis of positional deviation caused by position-dependent disturbances in ball screw drive. J Jpn Soc Precis Eng 2016;82(6):586–9.
[17] ISO. (2006), ISO 3408-5, Ball screws – Part 3: Acceptance conditions and acceptance tests.
[18] Shimoda H. Ball screw design analysis – part. 2 kinematic geometry of ball screw mechanism-. J Jpn Soc Des Eng 1991;26(11):516–9.
[19] ISO, (2006), ISO 3408-5, Ball screws – Part 5: Static and dynamic axial load ratings and operational life.
[20] Shimoda H. Stiffness analysis of ball screws. J Jpn Soc Precis Eng 1998;64(11):1581–4.
[21] THK CO., LTD. Product Descriptions Types of ball screw A15-22, https://tech.thk.com/en/products/pdf/en_a15_011.pdf#10.